Climate Dynamics (2019) 52:4143–4156
https://doi.org/10.1007/s00382-018-4372-3

Effects of background state on tropical cyclone size over the Western North Pacific and Northern Atlantic

Chen Ma[1] · Melinda Peng[2] · Tim Li[1,3] · Yuan Sun[4] · Jia Liu[1] · Mingyu Bi[1]

Received: 10 February 2018 / Accepted: 20 July 2018 / Published online: 31 July 2018

Abstract
Observational studies have shown that tropical cyclone (TC) size, commonly measured by the radius of the 17 m s^{-1} surface wind speed, in the western North Pacific (WNP) is statistically larger than its counterpart in the North Atlantic (NA). In this study we conduct idealized simulations for TC developments using high-resolution WRF model to understand the reason behind the size difference and relative contributions from among temperature, moisture and wind fields to modulate the TC size. Climatological mean states of the WNP and NA were computed using long-term analysis fields and used as background fields for the simulations. With identical initial vortices, TCs in the WNP environment evolve to larger sizes than those in the NA environment, consistent with previous observational studies and our own analysis using best track data. Experiments were designed to separate impacts of the specific humidity, wind fields, and the temperature profiles. Our simulations indicate that the temperature profile is the dominant factor in controlling the TC size with its influence about twice larger than from the specific humidity or the wind fields. The background climatological state in the WNP has a higher SST and a lower tropopause temperature than in the NA. This condition is favorable for more intense TCs. As the size is proportional to the intensity of the storm, this more unstable atmospheric condition is the reason behind the larger size observed in the WNP. The size of the inner core, represented by the radius of the maximum wind, settled down quickly in the early stage and is less correlated to the evolution of the outer size which continues to increase with the intensity increasing. The more favorable condition for the TC development and larger size in the WNP also correspond to the larger surface entropy flux.

1 Introduction

The size of a tropical cyclone (TC) is an important parameter to estimate how large the area its impact will be. The size of a TC, referred as the outer size instead of the inner-core size here, also will determine potential interactions with its nearby features and surrounding environments. Fiorino and Elsberry (1989) showed that TC size can influence the TC motion. Price (1981) pointed out that TC size can affect the ocean upwelling under the TC. Irish et al. (2008) found that storm surge will vary by 30% over a reasonable range of TC size for a given TC intensity. The climatology of TC sizes in past decades has been well studied, particularly over the western North Pacific (WNP) and North Atlantic (NA) (Merrill 1984; Kimball and Mulekar 2004; Chavas and Emanuel 2010; Chan and Chan 2012; Kim et al. 2014).

We conducted our own analysis of the statistical climatology for the size of TCs occurred over the WNP and NA from 2001 to 2010 based on the Joint Typhoon Warning Center (JTWC) and National Hurricane Center (NHC) data (Table 1). The result shows that TC size over the WNP is larger than that over the NA for both the mean and the median, consistent with the results of Chan and Chan (2012) in which the QuikSCAT data were used. Question remains on why there is such a size difference between these two basins? It might be expected that the mean states over the two oceans are different. In addition,

✉ Chen Ma
nuist-machen@foxmail.com

[1] Key Laboratory of Meteorological Disaster, Ministry of Education (KLME)/Joint International Research Laboratory of Climate and Environmental Change (ILCEC)/Collaborative Innovation Center on Forecast and Evaluation of Meteorological Disasters (CIC-FEMD), Nanjing University of Information Science and Technology, Nanjing, China

[2] GD-IT/Naval Research Laboratory, Monterey, CA, USA

[3] International Pacific Research Center and Department of Atmospheric Sciences, School of Ocean and Earth Science and Technology, University of Hawaii, Honolulu, HI, USA

[4] College of Meteorology and Oceanography, National University of Defense Technology, Nanjing 21101, China

Table 1 Observational statistics of R17 for the WNP and NA TCs from 2001 to 2010

	Basin	
	WNP	NA
No. of TCs	214	156
Average (km)	194.29	179.82
Median (km)	185.2	152.79

approximately 70–80% of TCs develop from tropical disturbances within the monsoon trough in the WNP (Molinari and Vollaro 2013); while the majority of TCs develop from easterly waves in the NA (Avila 1991; Avila and Pasch 1995; Landsea 1993). Previous studies also alluded that TC size is different in different ocean basins, years, latitudes, environmental humidities, environmental pressures, and with different minimum central pressures (Atkinson 1971; Frank and Gray 1980; Merrill 1984; Cocks and Gray 2002; Kimball and Mulekar 2004). For example, Merrill (1984) suggested that different latitudes and synoptic environments can lead to different TC sizes. Liu and Chan (2002) showed that the size of a TC depends on the nearby synoptic flow patterns. Hill and Lackmann (2009) found that environmental relative humidity is one factor controlling the TC size. Wang (2009) noted that heating and cooling in outer bands had an effect on the intensity and structure of TCs including the size of the storms. Emanuel (1986) indicated that the size of the initial disturbance can affect the final TC size. Smith et al. (2011) investigated the planetary rotational influences on TC size and intensity and have identified an intermediate Coriolis parameter with the optimal planetary vorticity for the strongest vortex and largest size. Knaff et al. (2014) used satellite images to investigate the TC size distribution globally. It was found that the TCs in the NA may continue to grow after reaching maximum intensity and TCs in the WNP have the largest size distribution in the world.

While some studies have presented relations between the TC size and some environmental conditions, the relative contribution of different dynamic and thermodynamic variables to modulate the TC size is not clear. In this study, through a series of idealized simulations, we will investigate how differences in the mean states in WNP and NA may lead to differences in the TC size and relative contributions from different variables to it.

The rest of this paper is organized as follows. The model configuration, climatological mean states of WNP and NA, initial vortex, and experimental design are given in Sect. 2. In Sect. 3, results from control experiments with the climatological mean states are examined. The relative roles of variables in the environmental state on determining the TC size are examined with additional experiments in Sect. 4. Finally, major findings of the study are summarized and discussed in Sect. 5.

2 The model and experiment design

2.1 Model configuration

The numerical model used in this study is the Advanced Research Weather Research and Forecasting (WRF-ARW) system, Version 3.3, (Skamarock et al. 2008). Three nested domains with the two inner nests having two-way interactions are constructed. For experiments in the WNP, the mesh sizes in the three domains are 300×250, 301×301, and 301×301, respectively. For experiments in the NA, the mesh sizes in the three domains are 278×160, 151×151, and 301×301, as the size of the NA is smaller than the WNP. The horizontal grid sizes of 27, 9, 3 km and vertical resolution of 46 vertical layers with a model top of 10 hPa are the same for both basins. The Kain-Fritch convective scheme (1993) is applied to the two outermost meshes and an explicit microphysics scheme (Lin et al. 1983) is used in all meshes. Other model physics include the Yonsei University (YSU) planetary boundary layer (PBL) scheme, thermal diffusion land surface scheme, and Monin–Obukhov surface-layer scheme (Hong et al. 2006). A fixed lateral boundary condition is used for the outermost domain and the two inner nested domains move automatically following the model storm (Davis et al. 2008).

2.2 Climatological mean states of WNP and NA

To understand how the environment may influence the TC size, the climatological states of WNP and NA are constructed using the National Centers for Environmental Prediction (NCEP) reanalysis data (Kalnay et al. 1996), and used as initial and lateral boundary conditions. Our data analysis covers a period from 2001 to 2010 during July to September. Figure 1 shows the surface temperature and wind fields at 850 hPa in the WNP and NA. The sea surface temperature (SST) is more uniformly distributed in the WNP while the SST in the NA has a larger gradient in the east–west and north–south directions.

Merrill (1984) pointed out that in general the TC size varies with latitude; Chan and Chan (2013) illustrated the relationship between the absolute angular momentum (AAM) and the TC size. One part of the AAM, the earth angular momentum, is proportional to the Coriolis parameter. Due to the dependence of TC intensity and size on the latitude, we put the initial vortex at the same latitude in both basins to exclude the latitudinal effect.

The black box (6°–16°N, 135°–145°E) in Fig. 1a outlines the location of the initial vortex in WNP, which is located within the summer monsoon trough as it is the favorable region for TC developments in the WNP (Chen

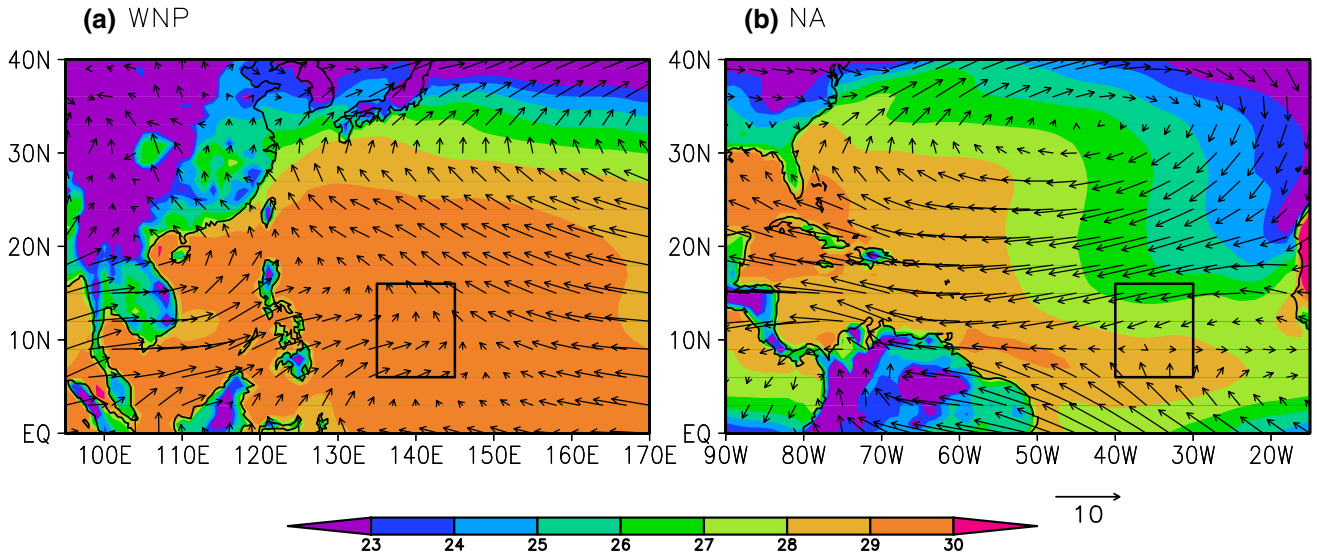

Fig. 1 Climatological summer surface temperature (shading in °C) and mean winds at 850 hPa (vector in m s^{-1}) from July–September for the period 2001–2010. The black box represents the area where the initial vortex is located

and Ding 1979; McBride 1995; Molinari and Vollaro 2013). In Fig. 1b, the initial vortex is placed in the box (6°–16°N, 30°–40°W) suitable for NA as most TCs originate from easterly waves off West African coast. Both black boxes in Fig. 1a, b contain more convergent flow in the wind fields, favoring the TC development.

2.3 Initial vortex

An axisymmetric weak vortex is placed at the center of the boxes shown in Fig. 1. The tangential wind of the initial vortex has the following radial and vertical profiles:

$$V_t(r,\sigma) = \begin{cases} \sin\left[\frac{\pi}{2}\left(\frac{\sigma-0.1}{1-0.1}\right)\right]\frac{V_m}{r_m}\left(e^{\left(1-\frac{r}{r_m}\right)} - \frac{|r-r_m|}{r_0-r_m}e^{\left(1-\frac{r_0}{r_m}\right)}\right) & \sigma > 0.1 \\ 0 & \sigma \leqslant 0.1 \end{cases}$$

where r is the radial distance from the vortex center, r_m the radius of maximum tangential wind, V_m the maximum tangential wind at the radius of r_m, σ the vertical sigma level and r_0 is 1000 km from the vortex center where the tangential wind decreases to zero. The maximum tangential wind of the initial vortex is 15 m s^{-1} at the radius of 150 km at the surface as shown in Fig. 2. The wind speed decreases gradually upward. The initial vortex has a minimum sea level pressure (MSLP) of 1008 hPa. The mass and thermodynamic fields are derived based on the nonlinear balance equation so that the initial vortex satisfies both the hydrostatic and gradient wind balances (Wang 1995, 2001).

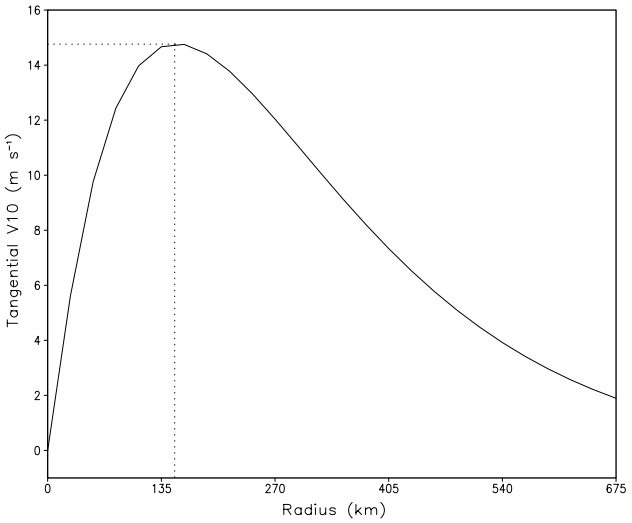

Fig. 2 The radial distribution of the azimuthal-mean tangential surface wind of the initial vortex in the simulation

2.4 Experimental design

Two control experiments were designed, one for the WNP and one for NA, identified as P_CTL and A_CTL, respectively (Table 2). The 10-year averaged summer mean state of WNP and NA including variable such as surface pressure, wind fields, geopotential height, temperature, SST, and specific humidity are used as the initial and lateral boundary conditions. Emanuel (1986) pointed out that the size of the initial disturbance can impact the final size of the TC. To avoid this complication, the initial vortices in all experiments have the same size and intensity. The experiment

Table 2 List of all experiments

Group	Wind	Temperature (including SST)	Specific humidity
P/A_CTL	Domain climatology	Domain climatology	Domain climatology
P/A_AVESH	Domain climatology	Domain climatology	2-domain average of zonal mean SH
P/A_NO_WND_CTL	None	2-domain average	2-domain average
P/A_NO_WND_T	None	Own domain average	2-domain average
P/A_NO_WND_SH	None	2-domain average	Own domain average

prefix of "P" or "A" denotes that the experiments are for WNP or NA, respectively.

Sensitivity experiments are conducted and results compared with the control experiments to identify impacts of different environmental parameters on the TC size. In the averaged specific humidity experiments (AVESH), the zonal mean specific humidity were averaged between the two oceans and used in the P_AVESH and A_AVESH experiments while other variables remain unmodified as in the control experiments. This set of experiment is designed to investigate the effect of moisture on the TC sizes. Meanwhile, the temperature and wind fields cannot be modified independently, because changing one variable will impact the other through thermal-wind relationship. Based on this consideration, three additional sets of experiments were designed. In the first group, identified as NO_WND_CTL experiments, the wind fields were set to zero, while other variables such as surface pressure, SST, geopotential height, temperature and specific humidity were set to the average of the two domain averages, varying only with height. In the second group, identified as NO_WND_T experiments, the wind fields are set to zero while the temperature profile is set to their own domain-averaged temperature in their respective regions with all other variables the same as in the NO_WND_CTL experiments. The temperature profiles shown and discussed below also include the SST as the temperature near the surface is directly related to the underlying SST. In the NO_WND_SH experiments, the specific humidity has its domain averages.

In summary, P_AVESH and A_AVESH have their own climate mean states except for the specific humidity, in which the average of the two domains is used. P_NO_WND_CTL and A_NO_WND_CTL have identical environment states and no winds. The only difference between them is the domain size, mainly the ocean part. P_NO_WND_T and A_NO_WND_T have their respective domain-averaged temperature profile, and P_NO_WND_SH and A_NO_WND_SH have their respective domain-averaged specific humidity, all with zero wind. The purpose of NO_WND_CTL, NO_WND_T and NO_WND_SH experiments is to find the relative influence on TC size from temperature profile and specific humidity differences. Then the remaining difference can be inferred that it is from the contribution of different wind fields. For each experiment, two parallel runs were conducted; one with an initial vortex and the other one without a vortex. The reason for having two parallel runs is to remove the evolution of the background fields when examining the evolution of the vortices. The difference between the two represents the evolution of the vortex under the influence of the background state. The figures shown and discussed below have all the fields from their respective parallel runs without a vortex subtracted off. All the experiments are listed in Table 2.

3 Effects of mean states on the TC size in WNP and NA

Figure 3 shows the simulated wind fields at the surface in the CTL experiments during the first three simulation days. With the same initial vortex, the one in the WNP background (P_CTL) is larger than that in the NA background states (A_CTL) for both the inner core and the outer radius. The vortex in the P_CTL is more symmetric than in the A_CTL, likely due to the more uniformly distributed SST and the mean flow (Fig. 1).

The average radius of the 17 m s^{-1} surface wind speed (R17) is a common measure of the TC size. We take two approaches to compute R17. One is the averaged size of the TC vortex from before and until 3 h after when it has reached its maximum intensity during the integration; the other is the average size of last 6 h of the simulation. In general, the two approaches produced similar results in term of the ratio between two pairs of the experiments for WNP and NA. Unless specified explicitly, the numbers using the first approach are displayed and discussed in the following, with numbers retrieved from both approaches listed in Table 3. Figure 4 compares the time evolution of the maximum wind speed (MWS) near the surface, the minimum sea level pressure (MSLP) and the size (R17) between P_CTL and A_CTL. The TC in P_CTL developed faster and became stronger than that in A_CTL. The evolutions of the R17 for P_CTL and A_CTL show that the size of TC in the WNP background is bigger than in the NA background (Fig. 4c). In general R17 gets larger as time evolves in numerical simulations. Kilroy et al. (2016) illustrated that the size of

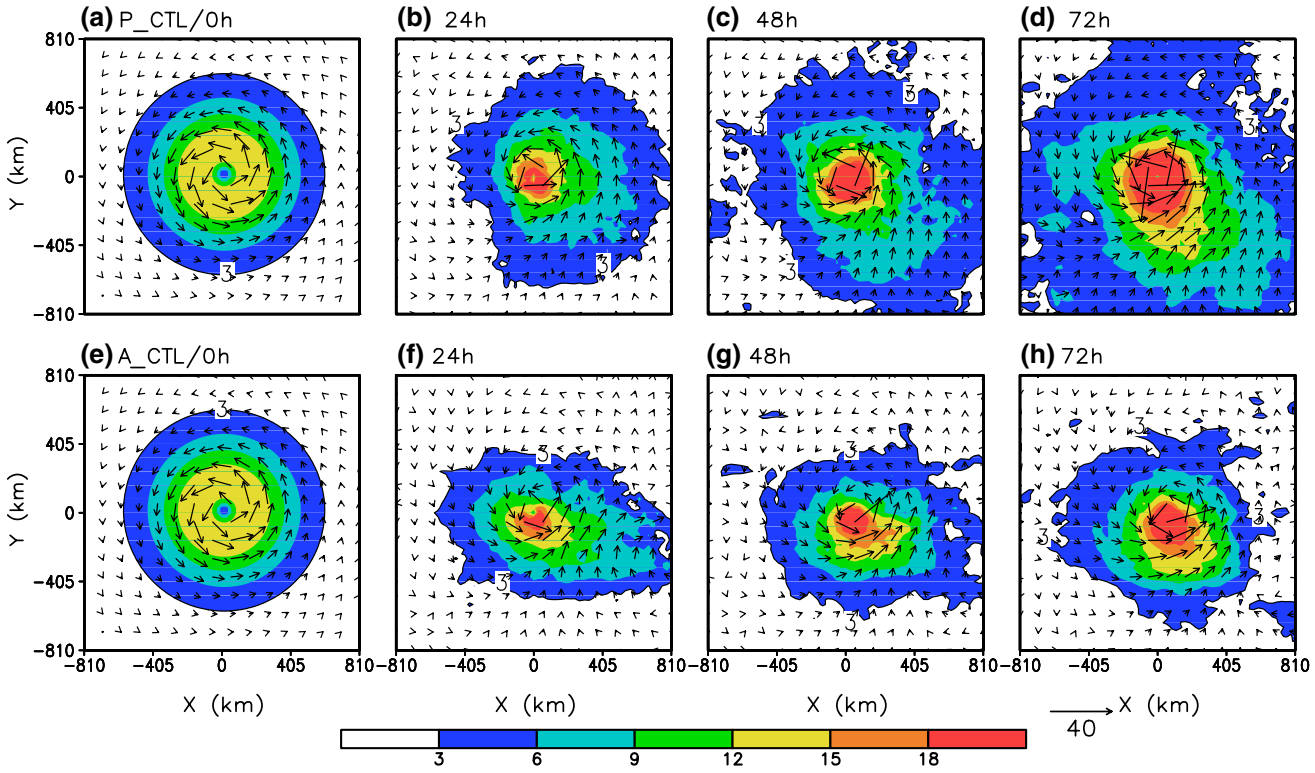

Fig. 3 Wind fields (vectors) and total wind speed (shaded) at surface in (**a**–**d**) P_CTL, and (**e**–**h**) A_CTL at the interval of 24 h

Table 3 The TC sizes (R17) in all experiments

Group	WNP (km)	NA (km)	ΔS (km)
CTL	165|184	114|114	51|70
AVESH	162|175	124|123	38|52
NO_WND_CTL	127|134	127|134	0
NO_WND_T	159|166	113|122	46|44
NO_WND_SH	141|142	119|121	22|21

The left-side number in a cell is the result from using the average size of the TC vortex before and after 3 h when it reached its maximum intensity. The right-side number in the cell is the result using the average size of the last 6 h of the simulation

a TC could continually increase even after the intensity has reached its maximum and begun decaying. Wu et al. (2015) constructed the relationship between TC size and intensity over the WNP using satellite images and concluded that the relationship is nonlinear. They found that the TC size generally increases with increasing TC maximum sustained wind before the TC size reaches 250 km or before the TC intensity reaches 53.0 m s^{-1} and then slowly decreases as the TC intensity further increases.

Figure 5 shows the radial distribution of the azimuthal-mean tangential wind at 10 m height for P_CTL and A_CTL in the TC mature stage. The average size of P_CTL

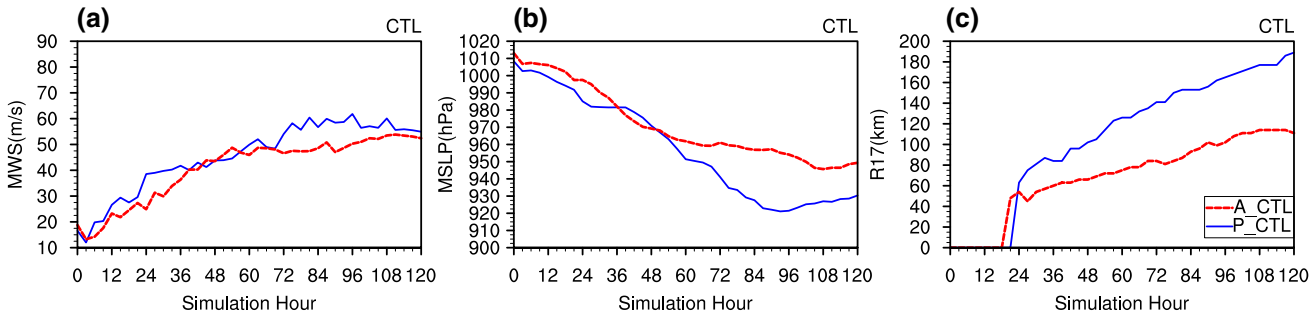

Fig. 4 Time evolutions of **a** MWS, **b** MSLP and **c** R17 at 10 m for P_CTL (blue line) and A_CTL (red line)

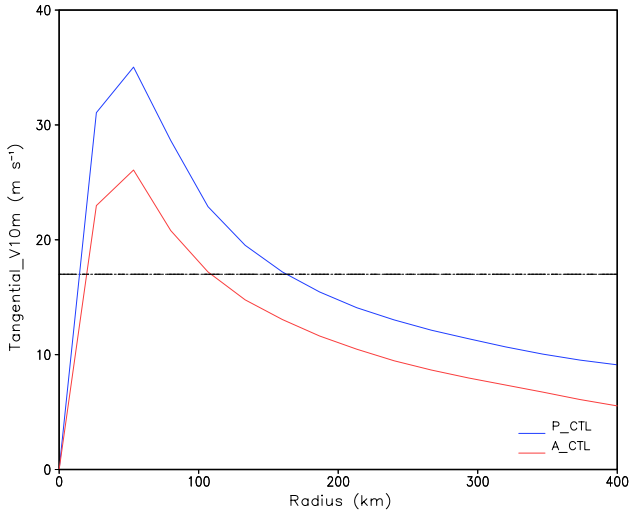

Fig. 5 The radial distribution of the azimuthal-mean tangential wind at 10 m height for P_CTL (blue) and A_CTL (red) in the TC mature stage. The dashed line denotes 17 m s^{-1}

and A_CTL as measured by R17 is 165 and 114 km, respectively, and the size difference is 51 km (Table 3). The size difference continues to increase, reaching about 70 km toward the end of simulation. This result of a larger TC size in the WNP than in NA is consistent with previous observational analyses (e.g., Chan and Chan 2012; Merrill 1984).

4 Contributions of different environmental variables to TC sizes

Next, we conduct sensitivity experiments to investigate the relative role of different environmental variables in affecting the TC size. Table 2 lists all the experiments designed to investigate separately the effect of specific humidity, temperature profile and wind fields on TC size.

4.1 Specific humidity

In the AVESH experiments, the specific humidity in the P_AVESH and A_AVESH are the same, using the average of the zonal mean specific humidity of the two ocean domains. Figure 6 shows the time evolutions of the simulated MWS, MSLP, and R17 in the experiments. Compared to the CTL, the TC size difference between WNP and NA is smaller in this set of experiment, as we have decreased moisture in WNP and increased moisture in NA by using the average between them. Values centered around the peak intensity at t = 114 h were used to compute the mature stage size in P_AVESH and t = 96 h for A_AVESH, and the retrieved values are 162 and 124 km, respectively, with a 38 km difference (Table 3). Comparing the R17 difference in the AVESH experiments (38 km) and the difference in the CTL experiments (51 km), we can estimate the contribution from different specific humidity. Since the specific humidity fields in the two AVESH experiments are the same, the 38 km size difference would come from the impact of other variables and the remaining 13 km difference (51 minus 38 km) can be attributed to the effect of specific humidity. Through the AVESH sensitivity experiments, the relative contribution of the specific humidity (SH) and all other state variables (NOSH) are shown in Fig. 7. Using percentage contribution, we arrive at a roughly 25% contribution from the specific humidity and 75% from other variables contributing to the TC size difference between WNP and NA (red bars in Fig. 7). Similar percentages are obtained using the final hour estimate of the size (blue bars in Fig. 7).

4.2 Temperature profile and wind fields

As the temperature field can be expressed as $T(x, y, p) = \overline{T}(p) + T'(x, y, p)$, it is necessary to point out that the temperature profile we refer to here is the stability-related vertical profile $\overline{T}(p)$ instead of disturbance part. In order to estimate the relative contributions of the temperature profile and the wind fields separately, three sets of experiments are conducted, listed in Table 2. In the first set

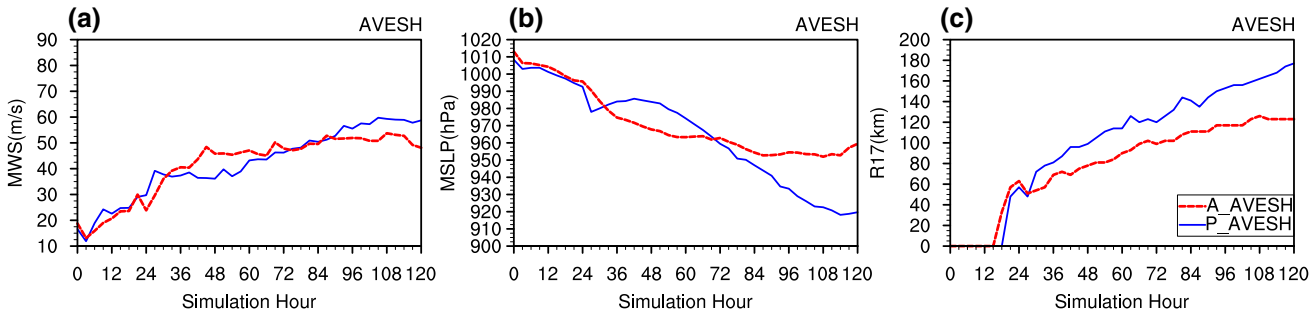

Fig. 6 Time evolutions of: **a** MWS, **b** MSLP and **c** R17 for the AVESH experiments

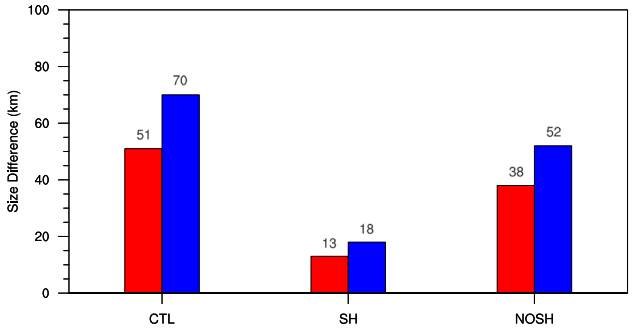

Fig. 7 Relative differences of the TC sizes in the WNP and NA: In the control with all the background states, contribution from the specific humidity difference (SH) and from the remaining state variables (NOSH). The red bar is the result using the averaged TC size from before and after 3 h when it reached its maximum intensity. The blue bar is the result using the averaged TC size of the last 6 h of simulation time

of experiment, the wind fields are set to zero and other variables (i.e. hgt, t, sh, ps, SST) are replaced by the average of two ocean domain-averaged vertical profiles, identified as NO_WND_CTL experiment, to isolate the effect of temperature and wind field. Since the SST in WNP is more uniform while that of NA has a larger meridional gradient (Fig. 1), we check the TC tracks of CTL experiments to ensure the TC difference is not caused by the local SST as the vortex moves during the integration. Figure 8 shows the TC tracks in WNP and NA for the CTL experiments and all sensitivity experiments. The track of A_CTL and A_AVESH in Fig. 8b moves almost with the constant background wind speed. The TCs in the other three experiments with no wind move with the beta effect to northwestward.

With identical environmental conditions except for the domain, the TC vortices in the NO_WND_CTL experiments are very similar, and are more symmetric and develop slightly slower than those in the CTL experiments (figures not shown). Figure 9a–c show the time evolutions of MWS, MSLP, and R17, respectively. The time chosen for computing the size around their lowest MSLP point is at 108 h for both P_NO_WND_CTL and A_NO_WND_CTL. The 6 h averaged sizes are nearly identical (Table 3). To demonstrate that the NO_WND experiments can serve our purpose without causing significant imbalance, we also conducted a supplemental experiment in which the wind fields are set to zero while all other environmental variables have their own domain averages. This supplemental experiment produced very similar evolutions of the intensity and size as in the control (figure not shown), and the size difference is 77 vs 70 km in the control.

In the NO_WND_T experiments, the domain averaged temperature profile in each basin is used for WNP and NA with zero winds and we compare them with the NO_WND_CTL experiments. Before we examine the TC sizes, the effect of temperature profile on TC intensity is assessed first since the TC size may be associated with the intensity (Wu et al. 2015). Figure 10a shows the temperature profile of P_NO_WND_T and A_NO_WND_T, where the tropopause in the simulations is around 17 km as reflected by the temperature inversion. Even though the temperature profiles look close to each other, the difference between them is more pronounced (Fig. 10c). The temperature in P_NO_WND_T is 1.5 degree warmer than in A_NO_WND_T near the surface while it is 1.5 degree colder at the tropopause. Emanuel (1988) proposed that the heat budget of a tropical cyclone can be considered as a Carnot engine with the thermal energy imported from the underlying ocean and exported in the upper-level outflow layer. The thermodynamic efficiency of a TC can thus be defined as $\varepsilon = \frac{T_s - T_0}{T_s}$ from the environmental temperature where T_s is the temperature at the bottom

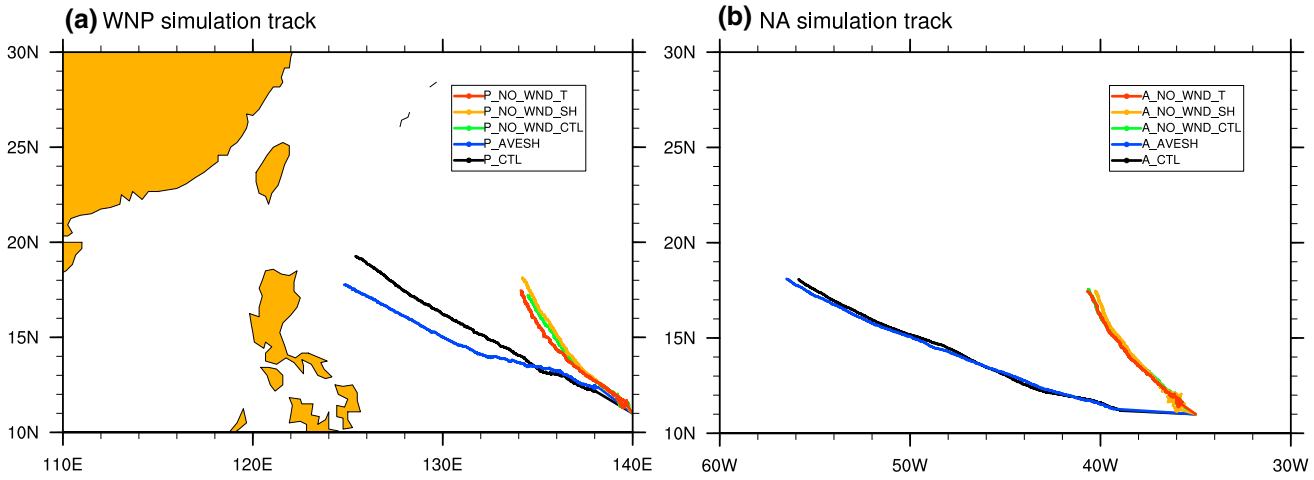

Fig. 8 Strom tracks of all experiments in **a** WNP and **b** NA

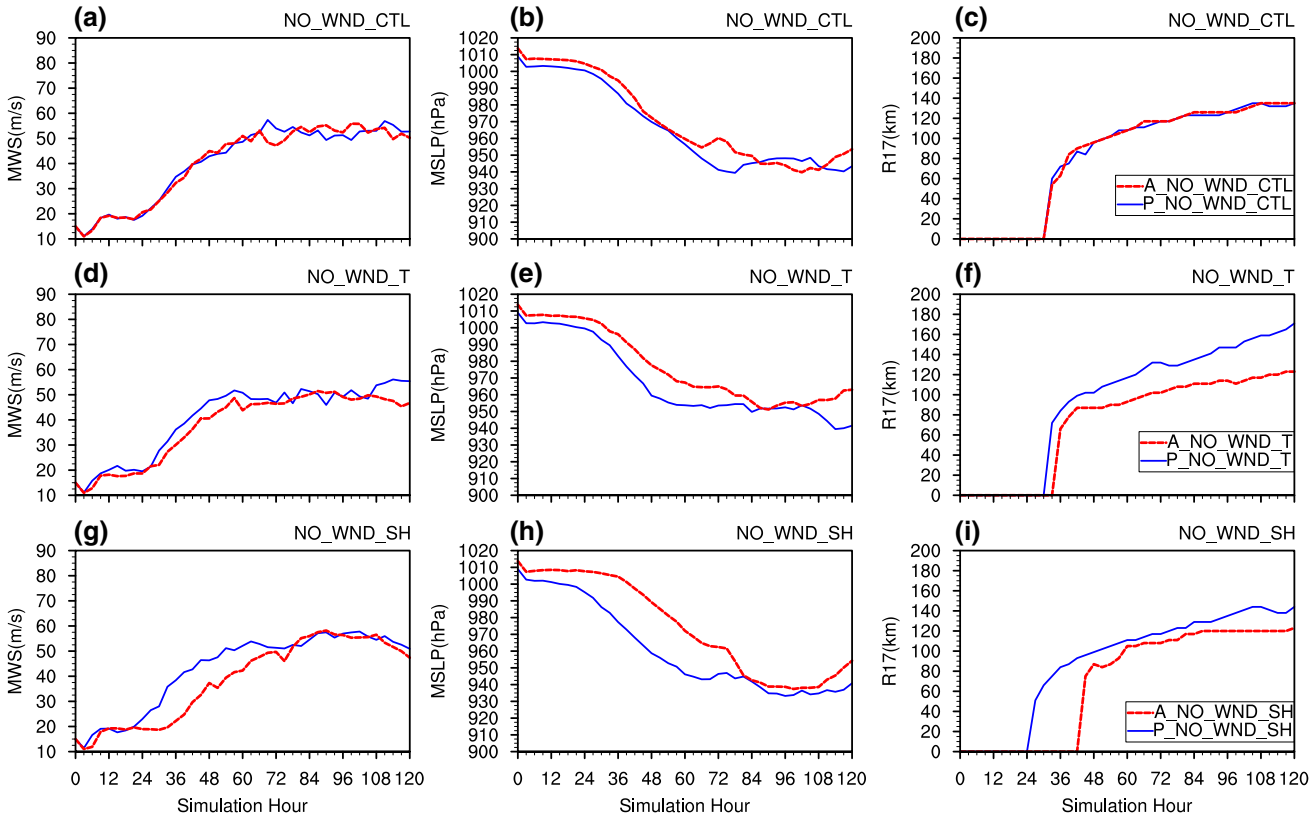

Fig. 9 Time evolutions of the MWS (left), MSLP (center) and R17 (right) of NO_WND_CTL experiments (**a**–**c**, upper panels); NO_WND_T experiments (**d**–**f**, middle panels); and NO_WND_SH experiments (**g**–**i**, lower panels)

and T_o is the temperature at the top. Based on the temperature profiles in the two ocean basins, the (T_s–T_o) in the WNP is about 3 degrees larger than in the NA. In other words, the temperature profile of WNP is more favorable for the higher TC intensity.

Since the temperature difference between the top and the bottom is larger in the WNP, the intensity of P_NO_WND_T experiment is higher so that the MSLP is lower than in A_NO_WND_T (Fig. 9e). In this set of experiment, the 6 h averaged size of R17 is 159 km for P_NO_WND_T and 113 km for A_NO_WND_T, with the time for estimating the TC mature-stage average size at 112 and 90 h, respectively (Fig. 9f). The mature stage size difference between them is 46 km (Table 3). Since the only difference in these two NO_WND_T experiments is the temperature profile, this size difference comes from the temperature difference.

The moisture of the background state can also affect the TC size as discussed in Sect. 4.1. Figure 10b, d show profiles and difference of the specific humidity in P_NO_WND_SH and A_NO_WND_SH. In this set of experiment, the temperature profiles used are the same as the average between the two basins while the specific humidity holds its own domain-average. The specific humidity of the WNP is more abundant at almost every level. Figure 9g–i show the time evolutions of MSLP, MWS and R17 in the NO_WND_SH experiments. The TC-vortex in A_NO_WND_SH developed later than in P_NO_WND_SH so that the size difference between them is large in the early stage. The late development of the TC-vortex in A_NO_WND_SH is also shown by the size expansion of the vortex as measured by R17 (Fig. 9i).

The result indicates that more abundant specific humidity in WNP can make the TC size larger (Fig. 9i). The instantaneous rainfall rates are plotted in Figs. 11 and 12 for the NO_WND_T and NO_WND_SH, respectively. While the intensity of the rainfall rates corresponds well with the TC intensities, the rainfall distributions are more similar in the NO_WND_SH than in the NO_WND_T experiment. Compared with NO_WND_SH, the difference in area of TC spiral rain band is larger in NO_WND_T, which indicates that the difference in TC size is also more obvious. The model is capable of simulating spiral rainband in the absence of background winds. In the P_NO_WND_T experiment (Fig. 11), the rainband is larger and contracts toward the inner core, potentially with eyewall replacement mechanism. In the A_NO_WND_T experiment, the precipitation is more confined near the core. The delayed development in A_NO_WND_SH comparing with P_NO_WND_SH can

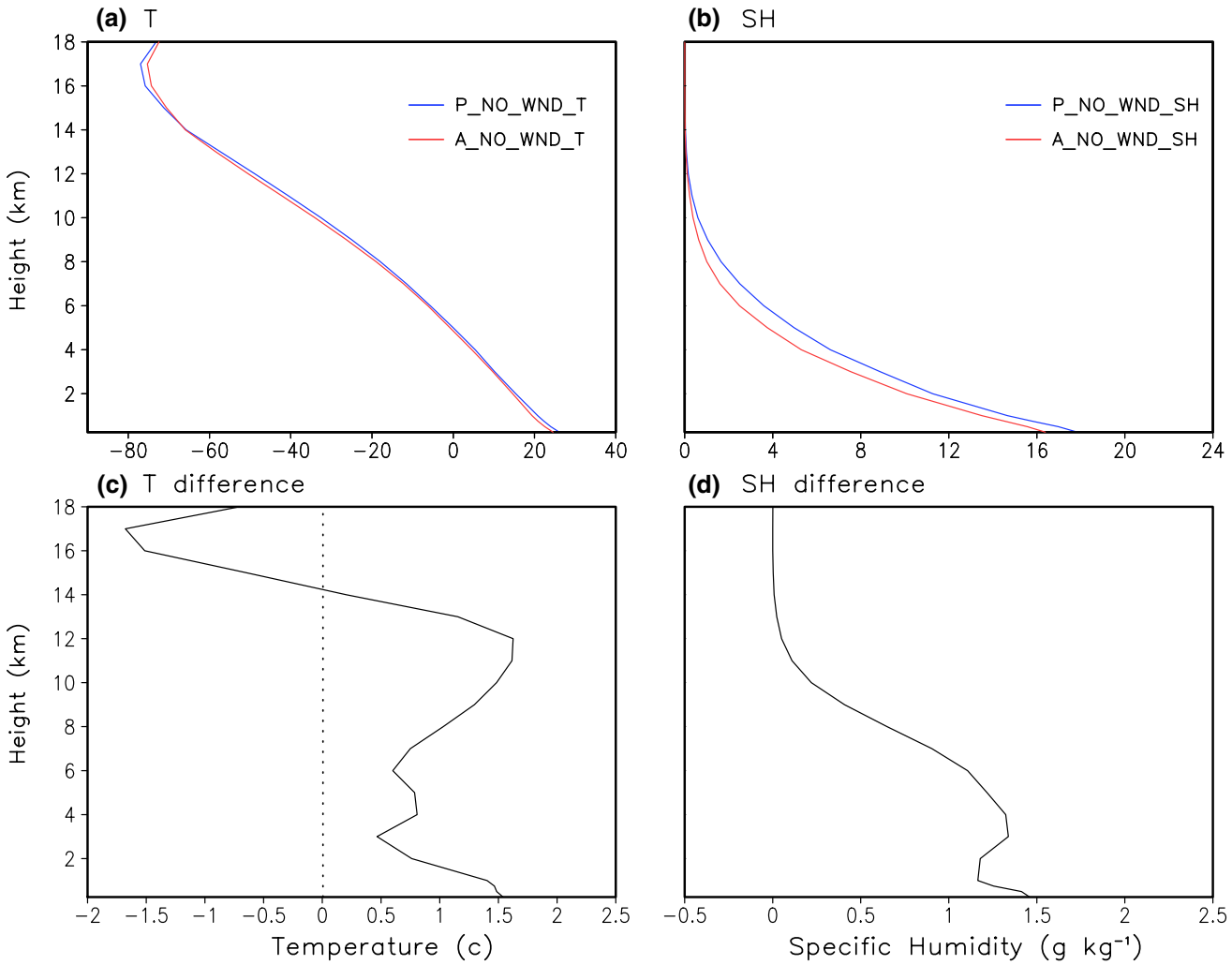

Fig. 10 The vertical profiles of the domain-averaged **a** temperature profile and **b** specific humidity of WNP (blue) and NA (red). **c, d** Are the difference of the vertical temperature profile and specific humidity between WNP and NA

also be seen from the rainfall rate distribution (Fig. 12). The time for computing the size at the mature stage chosen for P_NO_WND_SH and A_NO_WND_SH is at 102 and 96 h and the 6-h averaged mature stage size is 141 and 119 km, respectively.

From the result of these three sets of experiments, we estimated that the contribution of temperature profile and specific humidity on TC size has a ratio of about 2.1:1, between the size difference from NO_WND_T (46 km) and the size difference from NO_WND_SH (22 km). In Sect. 4.1, we have deduced that the impact of specific humidity to the TC size is about 25–26%. Using the relationship of 2.1:1 between the contribution from temperature profile and from the specific humidity, we then arrive at a 53–55% contribution from the temperature profile. The remaining percentage of the TC size difference is about 19–22% that can be inferred as the contribution from the wind field differences (Fig. 13).

4.3 Possible mechanisms for the difference of R17

From the point of view of the TC tangential wind profile, R17 is related to storm inner-core size represented by the radius of maximum wind (RMW), the slope of tangential winds outside the RMW, and the intensity of TC (MWS). In order to find the possible mechanism for the R17 difference between the two basins investigated here, we first collect the R17 and MWS data from all experiments beyond the 24 h integration (Fig. 14a, b). Lines represents linear regression and r is the slope of the line. The correlation coefficient between R17 and MWS is 0.81 for all experiments including both basins. The high correlation between the size and the intensity is resonable because the R17 is the distance that the wind decays to gale force from the TC center. In other words, the stronger the MWS, the larger the R17, and vice versa (Wu et al. 2015; Knaff et al. 2015).

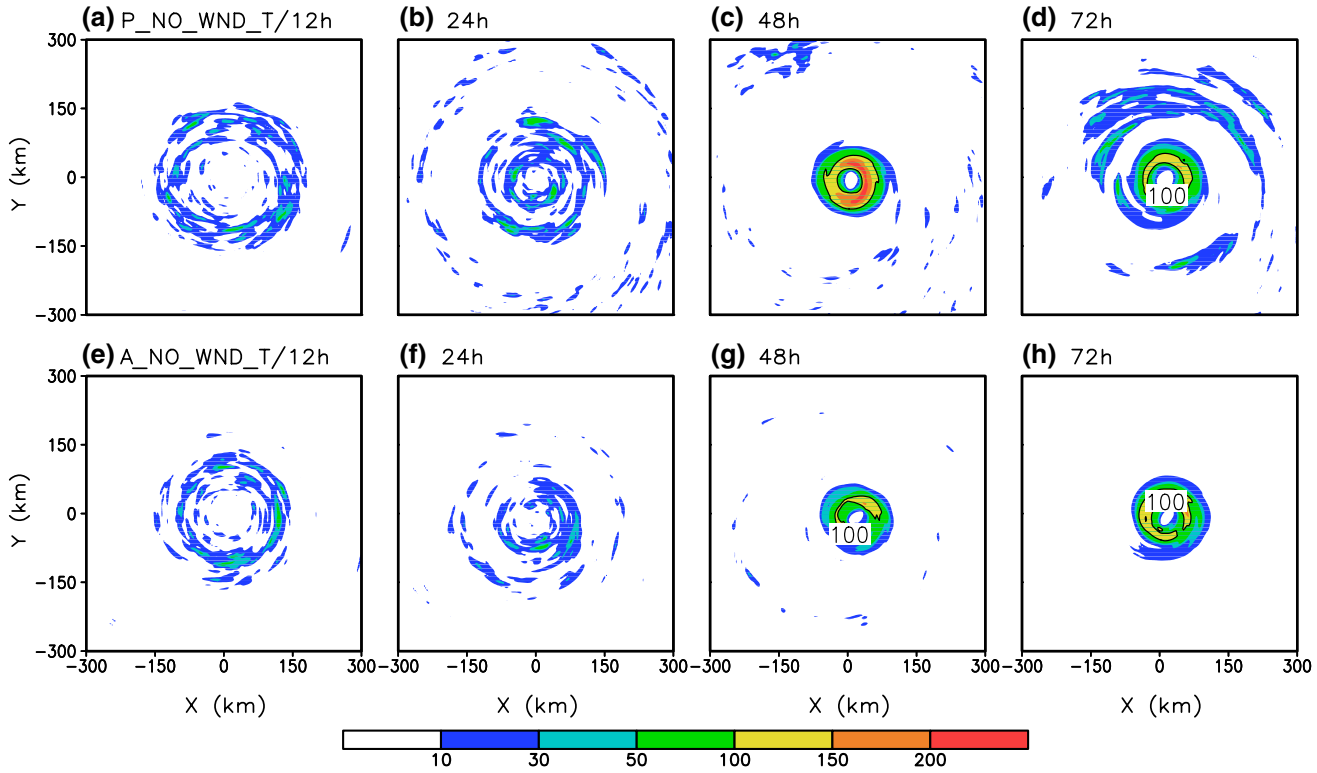

Fig. 11 Plots of instantaneous rainfall rate (mm h^{-1}) including cumulus and grid scale precipitation in (**a**–**d**) for P_NO_WND_T, and (**e**–**h**) for A_NO_WND_T

Comparing the two panels, TCs in the WNP have larger R17 than those in the NA with similar intensities.

The relationship between R17 and RMW is displayed in Fig. 14c, d for the WNP and NA, respectively. The correlation coefficient between the RMW and R17 is 0.62. This number is less than the one between R17 and MWS as in some experiments RMW contracts while the intensity and R17 increases. In addition, there are situations where R17 of the WNP TCs are larger than in the NA with similar inner-core size.

Xu and Wang (2010) pointed out that the surface entropy fluxes (SEF) are critical to the growth of the inner-core size. SEF is the sum of sensible-heat and latent-heat flux. Here we explore the relationship between SEF and the size difference. The time evolutions of the sizes along with SEF for all cases are plotted in Fig. 15. In Fig. 15a, b, the area-integrated SEF are computed within a 150 km radius. We also computed the SEF with different radial area, including 75 and 300 km. Their time evolutions are very similar to those shown here within the radius of 150 km (figures not shown). While the SEF increases steadily with time for both basins, the RMW of the simulated TCs contracted rapidly in the first 24–36 h with little changes thereafter (Fig. 15c, d). Meanwhile, the R17 increases gradually along with the increase of the SEF (Fig. 15e, f). The RMW of TCs is larger in the WNP than in the NA in a confined area near the core (Fig. 15c, d), and the averaged difference is roughly 6.5 km for all experiments. In summary, the inner-core size settles down quickly in the early stage without much further changes while the outer size continues to increase.

The TC intensities increase with the increase of the SEF as shown by the MSLP (Fig. 15g, h) and MWS (Fig. 15i, j) evolutions. The SEF in Fig. 15a, b indicates that the background state in the WNP generates more SEF than in the NA, leading to higher TC intensities in the WNP. Comparing to the difference of the RMW (Fig. 15c, d), the difference of the R17 (Fig. 15e, f) between the two basins is larger. The integrated SEF and the temperature profiles explain the difference in the intensity and R17 between TCs in WNP and NA.

There is no clear relationship between the SEF and its corresponding intensity and size for individual experiments within each basin. For example, the NO_WND_T has the largest SEF among the experimental group in the WNP, but neither its intensity nor its size stands out. We speculate that the vertical temperatrue profiles for individual cases such as displayed in Fig. 10 may shed some lights on the intensity differences. Since our current study is focused on the difference between the two basins, we have not exhausted the effort to investigate individual cases within each basin. The

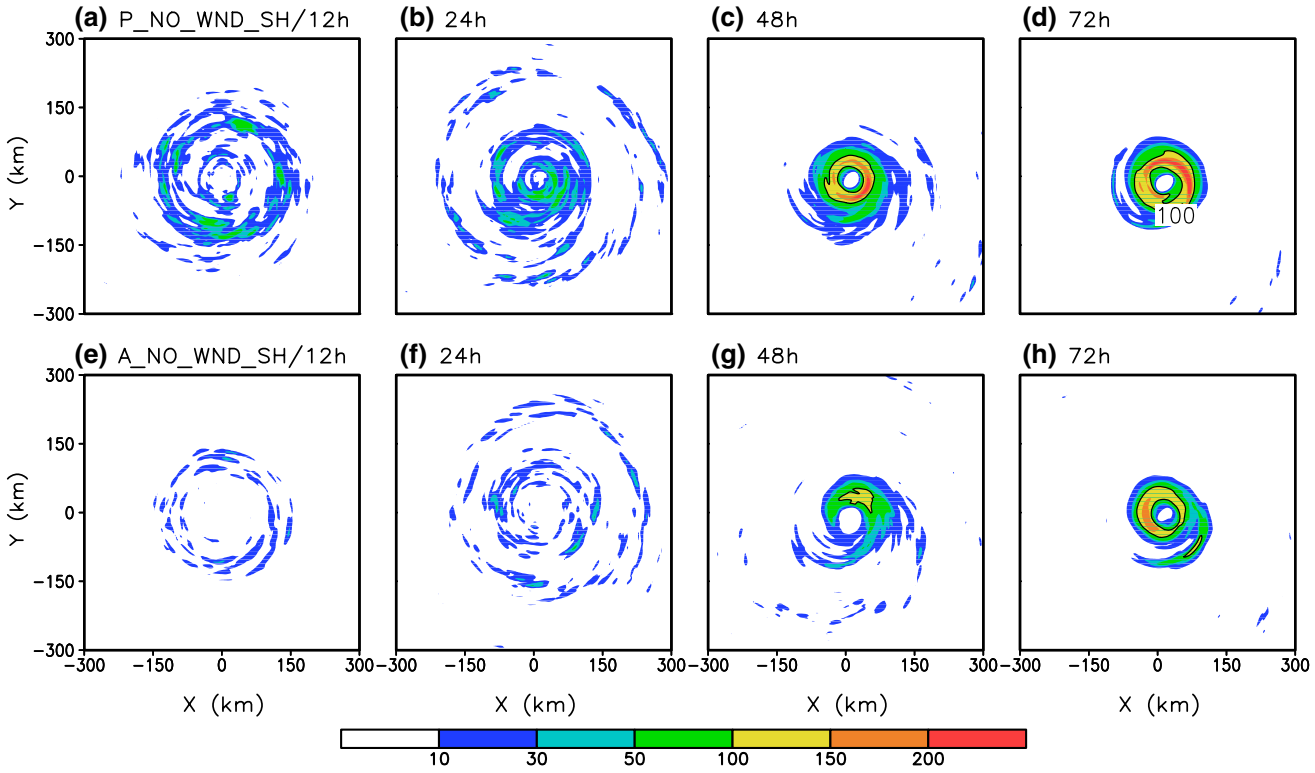

Fig. 12 Plots of the instantaneous rainfall rate (mm h^{-1}) including cumulus and grid scale precipitation in (**a**–**d**) P_NO_WND_SH, and (**e**–**h**) A_NO_WND_SH

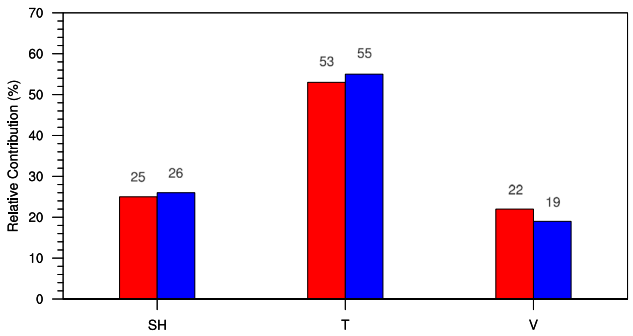

Fig. 13 Relative contribution of specific humidity, temperature profile and wind field to the TC size difference between WNP and NA. The red bar is the result using the averaged TC size from before and after 3 h when it reached its maximum intensity. The blue bar is the result using the averaged TC size of the last 6 h of simulation time

main conclusion is that the TC outer size depends on the TC intensity while the inner size does not increase with time.

5 Summary and discussion

Observational studies indicated that the outer sizes of TCs are different in different basins, years, latitudes, and environmental conditions. A clear characteristics is that TCs in the WNP in general have larger sizes than those in NA. It has not been well understood why the TC size difference exists between the WNP and NA and what environmental factor is more important in influencing the TC size. In this study, we conduct a series of idealized numerical experiments with the climatological mean states extracted from a long period of reanalysis data to investigate how the mean state affects the TC size. Through carefully designed experiments, we estimate the relative contribution of the temperature profile, specific humidity and wind fields to the size differences between the WNP and NA.

The control experiments using the climatology mean states of the two basins as the background show that the WNP state is more favorable for more intense TCs than the state of the NA. The outer size of a TC, as measured by the radius of the gale force wind, increases with the increase of

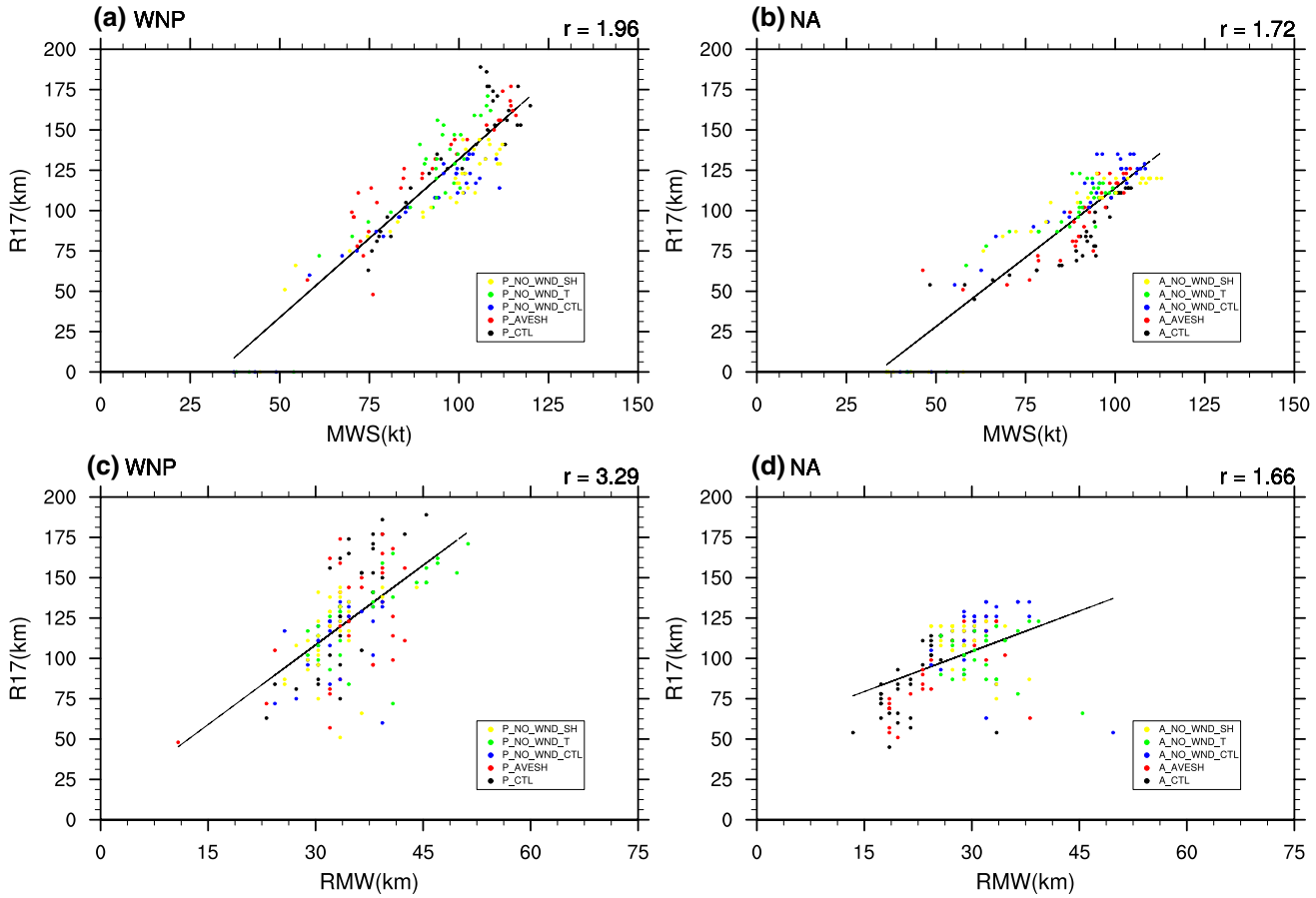

Fig. 14 Scatter diagrams for: R17 versus MWS (upper panels); and for R17 vesrus radius of maximum wind (lower panels). All model simlution data beyond 24 h are included from experiments for the WNP (left panels) and for the NA (right panels). Lines indicate the regression fit. The correlation coefficient between R17 and MWS is 0.81, and 0.62 between R17 and RMW

the TC intensity. A linear correlation between the intensity and the size is obtained. Therefore, a favorable environment for TC intensity is also supportive of larger TC sizes. The inner-core size, as measured by the radius of the maximum wind, collapses quickly during the early TC developing stage and then remains relatively unchanged as the TC continues to intensify. The temperature profile of the mean state in the WNP has a higher sea surface temperature and a lower tropopause temperature than in the NA. Based on the theory of Emanuel's Maximum potential intensity (MPI) theory, we identified that the temperature profile of WNP can support more intense TCs, leading to a larger size. The influence of the temperature profile to the TC size difference is about twice as large as humidity profile, the latter slightly more important than the wind fields. The intensity evolution also corresponds well with the surface entropy flux evolution. In summary, the larger TC sizes in the WNP are a result of higher TC intensities supported by its environment.

In the current study, we concentrate on the effect of the mean state on the TC size difference. In the future study, we will further examine the impact of initial disturbance on the TC size in different basins. In previous studies, it was identified that synoptic wave train is the major precursor disturbance for TCs in the WNP while it is the easterly waves in the NA. We will investigate how different pre-storm disturbances and interactions between the environment and the TC disturbances affect the TC sizes.

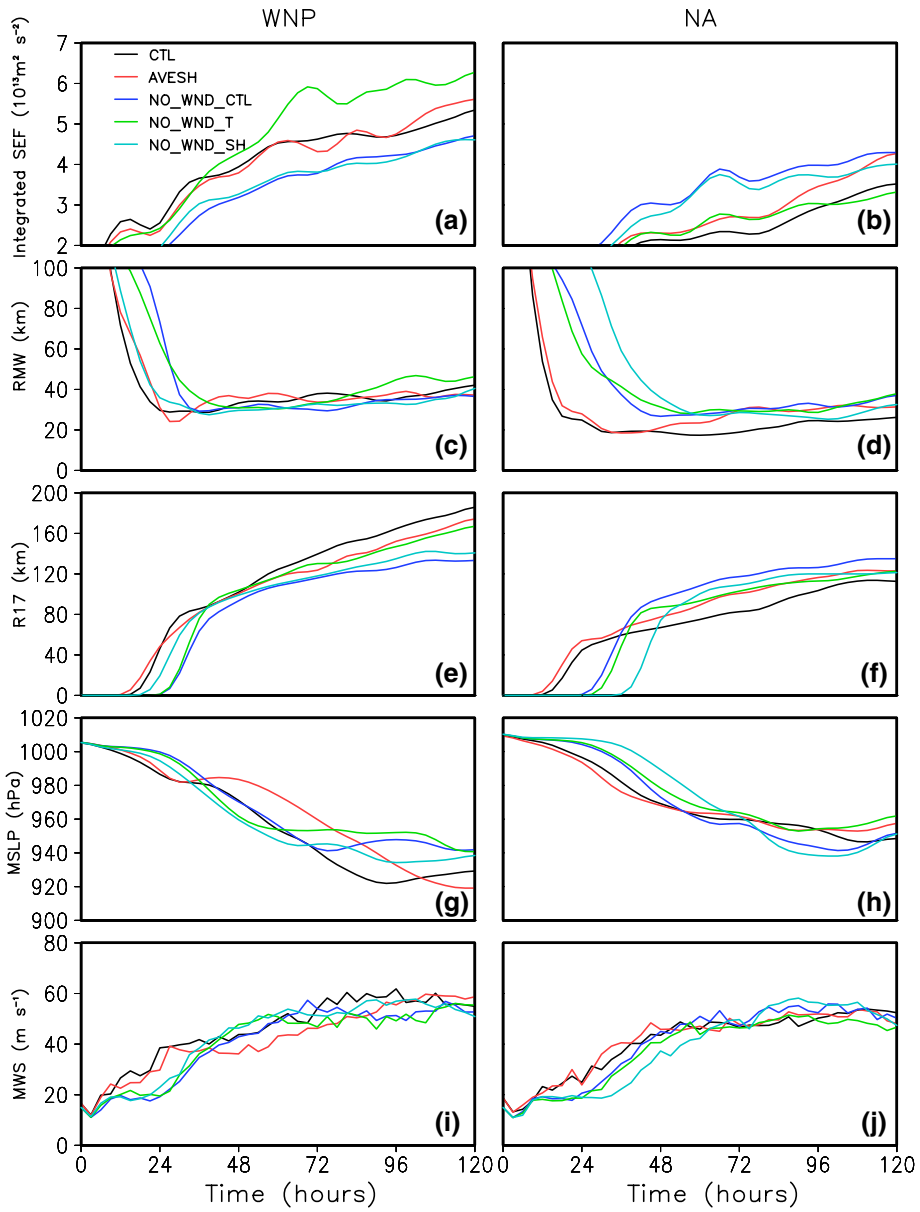

Fig. 15 Temporal evolutions for all experiments. **a, b**: area-integrated SEF (10^{13} m^2 s^{-2}) within a radius of 150 km; **c, d**: radius of maximum wind (RMW); **e, f**: the outer size, R17; **g, h**: MSLP; and **i, j**: maximum wind speed (MWS)

Acknowledgements This work was supported by China National Key R&D Program 2017YFA0603802 and 2015CB453200, NSF AGS-16-43297, NSFC Projects 41630423, 41475084 and 41575043, Jiangsu Projects BK20150062 and R2014SCT001, and the Priority Academic Program Development of Jiangsu Higher Education Institutions (PAPD). This is SOEST contribution number 10422, IPRC contribution number 1331, and ESMC contribution number 229.

References

Atkinson GD (1971) Forecaster's guide to tropical meteorology. Air Weather Serv Tech Rep 240, Scott Air Force Base, IL, p 295

Avila LA (1991) Atlantic tropical systems of 1990. Mon Weather Rev 119:2027–2033

Avila LA, Pasch RJ (1995) Atlantic tropical systems of 1993. Mon Weather Rev 123:887–896

Chan KTF, Chan JCL (2012) Size and strength of tropical cyclones as inferred from QuikSCAT data. Mon Weather Rev 140:811–824. https://doi.org/10.1175/MWR-D-10-05062.1

Chan KTF, Chan JCL (2013) Angular momentum transports and synoptic flow patterns associated with tropical cyclone size change. Mon Weather Rev 141:3985–4007. https://doi.org/10.1175/MWR-D-12-00204.1

Chavas DR, Emanuel KA (2010) A QuikSCAT climatology of tropical cyclone size. Geophys Res Lett 37:L18816. https://doi.org/10.1029/2010GL044558

Chen L, Ding Y (1979) The Conspectus of Western Pacific Typhoon. Science Press, Beijing 109 **(in Chinese)**

Cocks SB, Gray WM (2002) Variability of the outer wind profiles of western North Pacific typhoons: classifications and techniques for analysis and forecasting. Mon Weather Rev 130:1989–2005

Davis C et al (2008) Prediction of landfalling hurricanes with the advanced Hurricane WRF Model. Mon Weather Rev 136:1990–2005. https://doi.org/10.1175/2007MWR2085.1

Emanuel KA (1986) An air–sea interaction theory for tropical cyclones. Part I: steady-state maintenance. J Atmos Sci 43:585–604

Emanuel KA (1988) The maximum intensity of hurricanes. J Atmos Sci 45, 1143–1155, https://doi.org/10.1175/1520-0469(1988)045%3C1143:TMIOH%3E2.0.CO;2

Fiorino M, Elsberry RL (1989) Contributions to tropical cyclone motion by small, medium, and large scales in the initial vortex. Mon Weather Rev 117:721–727

Frank WM, Gray WM (1980) Radius and frequency of 15 (30 kt) winds around tropical cyclones. J Appl Meteorol 19:219–223

Hill KA, Lackmann GM (2009) Influence of environmental humidity ontropical cyclone size. Mon Weather Rev 137:3294–3315

Hong SY, Noh Y, Dudhia J (2006) A new vertical diffusion package with an explicit treatment of entrainment processes. Mon Weather Rev 134:2318–2341. https://doi.org/10.1175/MWR3199.1

Irish JL, Resio DT, Ratcliffe JJ (2008) The influence of storm size on hurricane surge. J Phys Oceanogr 38:2003–2013

Kain JS, Fritsch JM (1993) Convective parameterization for mesoscale models: the Kain–Fritsch scheme. Represent Cumulus Convect Numer Models Meteorol Monogr Am Meteorol Soc 46:165–170

Kalnay E et al. (1996) The NCEP/NCAR 40-year reanalysis project. Bull Am Meteorol Soc 77:437–471, https://doi.org/10.1175/1520-0477(1996)077%3C0437:TNYRP%3E2.0.CO;2

Kilroy G, Smith RK, Montgomery MT (2016) Why do model tropical cyclones grow progressively in size and decay in intensity after reaching maturity? J Atmos Sci 73:487–503. https://doi.org/10.1175/JAS-D-15-0157.1

Kim HS, Vecchi GA, Knutson TR, Anderson WG, Delworth TL, Rosati A, Zeng F (2014) Tropical cyclone simulation and response to CO_2 doubling in the GFDL CM2.5 high-resolution coupled climate model. J Clim 27:8034–8054. https://doi.org/10.1175/JCLI-D-13-00475.1

Kimball SK, Mulekar MS (2004) A 15-year climatology of North Atlantic tropical cyclones. Part I: size parameters. J Clim 17:3555–3575

Knaff JA, Longmore SP, Molenar DA (2014) An objective satellite-based tropical cyclone size climatology. J Clim 27:455–476. https://doi.org/10.1175/JCLI-D-13-00096.1

Knaff JA, Slocum CJ, Musgrave KD, Sampson CR, Strahl BR (2015) Using routinely available information to estimate tropical cyclone wind structure. Mon Weather Rev 144:1233–1247

Landsea CW (1993) A climatology of intense (or major) Atlantic hurricanes. Mon Weather Rev 121:1703–1713

Lin YL, Farley RD, Orville HD (1983) Bulk parameterization of the snow field in a cloud model. J Appl Meteorol 22:1065–1092, https://doi.org/10.1175/1520-0450(1983)022%3C1065:BPOTSF%3E2.0.CO;2

Liu KS, Chan JCL (2002) Synoptic flow patterns associated with small and large tropical cyclones over the western North Pacific. Mon Weather Rev 130:2134–2142

McBride JL (1995) Tropical cyclone formation. In: Elsberry RL (Ed) Global perspectives on tropical cyclones. World Meteorological Organization, Geneva, 63–105

Merrill RT (1984) A comparison of large and small tropical cyclones. Mon Weather Rev 112:1408–1418

Molinari J, Vollaro D (2013) What percentage of western North Pacific tropical cyclones form within the monsoon trough? Mon Weather Rev 141:499–505. https://doi.org/10.1175/MWR-D-12-00165.1

Price JF (1981) Upper ocean response to a hurricane. J Phys Oceanogr 11:153–175

Skamarock WC et al (2008) A description of the Advanced Research WRF version 3. NCAR Tech. Note NCAR/TN-4751STR, 113 pp

Smith RK, Schmidt CW, Montgomery MT (2011) An investigation of rotational influences on tropical-cyclone size and intensity. Quart J R Meteorol Soc 137:1841–1855. https://doi.org/10.1002/qj.862

Wang YQ (1995) On an inverse balance equation in sigma coordinates for model initialization. Mon Weather Rev 123:482–488, https://doi.org/10.1175/1520-0493(1995)123%3C0482:AIBEIS%3E2.0.CO;2

Wang YQ (2001) An explicit simulation of tropical cyclones with a triply nested movable mesh primitive equation model: TCM3. Part I: model description and control experiment. Mon Weather Rev 129:1370–1394, https://doi.org/10.1175/1520-0493(2001)129%3C1370:AESOTC%3E2.0.CO;2

Wang YQ (2009) How do outer spiral rainbands affect tropical cyclone structure and intensity? J Atmos Sci 66:1250–1273

Wu L, Tian W, Liu Q, Cao J (2015) Implications of the observed relationship between tropical cyclone size and intensity over the western North Pacific. J Clim 28:9501–9506

Xu J, Wang Y (2010) Sensitivity of tropical cyclone inner-core size and intensity to the radial distribution of surface entropy flux. J Atmos Sci 67:1831–1852